IEEE Access
Multidisciplinary | Rapid Review | Open Access Journal

Received February 20, 2019, accepted March 7, 2019, date of publication March 25, 2019, date of current version April 12, 2019.

Digital Object Identifier 10.1109/ACCESS.2019.2904287

Joint Estimation of the DOA and the Number of Sources for Wideband Signals Using Cyclic Correntropy

FANGXIAO JIN[1], TIANSHUANG QIU[1], SHENGYANG LUAN[2], (Member, IEEE), AND WEI CUI[3]

[1]Faculty of Electronic Information and Electrical Engineering, Dalian University of Technology, Dalian 116024, China
[2]School of Electrical Engineering and Automation, Jiangsu Normal University, Xuzhou 221116, China
[3]Neusoft Corporation, Dalian 116024, China

Corresponding author: Tianshuang Qiu (qiutsh@dlut.edu.cn)

This work was supported by the Nature Science Foundation of China (NSFC) under Grant 61671105, Grant 61139001, Grant 61172108, Grant 61801197, and Grant 81241059.

ABSTRACT In this paper, a new direction of arrival (DOA) and the number of signals of interest (SOIs) estimation method is proposed for wideband sources in impulsive noise environments. By evaluating the cyclic correntropy function (CCF) of the received signals at a certain cycle frequency, the impulsive noise and all co-channel interferences with different cycle frequencies can be suppressed. In this approach, a theorem of the CCF is proposed, and a linear prediction (LP) model of the CCF of the array data, which is important for both DOA and number of SOIs estimations, is built by the theorem. Additionally, we introduce multiple regularization parameters into the LP model and derive an analytical expression of the maximum correntropy criterion (MCC) of the parameters for obtaining the optimal regularization parameters expression. Furthermore, by the expression of regularization parameters and the estimation error of the CCF in a limited number of snapshots, an iterative algorithm is proposed for joint estimation of the DOA and the number of SOIs with only knowledge of the cycle frequency of the SOIs.

INDEX TERMS Wideband sources, direction of arrival (DOA), cyclic correntropy function (CCF), maximum correntropy criterion (MCC).

I. INTRODUCTION

The estimation of the direction of arrival (DOA) is an important aspect of array signal processing. The goal is to determine the geometric position information of signals in the same spatial region. This estimation is widely used in radar, sonar, communication, passive detection and other fields [1]. In general, the subspace-based methods to estimate the DOA of narrowband signals, such as MUSIC [2], ESPRIT [3], Min-Norm linear prediction (LP) [4], and the method of direction estimation (MODE) [5], are well-known because of their low computational complexity and high resolution capability.

These classical DOA algorithms are mainly based on the Gaussian noise assumption. The performance of the algorithms will degrade or even fail in the presence of a non-Gaussian noise. However, in practice, the noise often exhibits non-Gaussian properties. One important class of non-Gaussian noises is the impulsive noise, which is characterized by sudden bursts or sharp spikes and is frequently encountered in many practical wireless radio systems [6]. A number of DOA estimation methods in impulsive noise have been proposed. A class of subspace based DOA estimation algorithms uses the fractional lower-order statistics (FLOS) instead of the second-order sample covariance, such as the robust covariation-based MUSIC (ROC-MUSIC) [7], fractional lower-order moments in FLOM-MUSIC [8], Kendall's tau covariance matrix in TCM-MUSIC [9], etc. Furthermore, for the DOA estimation of wideband signals with impulsive noise, a new subspace-based method based on the geometrical properties of the data model was presented in [10]. In [11], based on the characteristics of impulsive noise, You *et al.* presented a fast DOA estimation algorithm by the fractional lower-order cyclic correlation function.

Universally, these DOA estimation methods require a priori knowledge of the number of the signals, which is one of the more critical and difficult problems facing passive sensor arrays systems. To solve this problem, the weight subspace fitting (WSF) algorithm [12], [13] is used for sensor

The associate editor coordinating the review of this manuscript and approving it for publication was Ahmet M. Elbir.

2169-3536 © 2019 IEEE. Translations and content mining are permitted for academic research only.
Personal use is also permitted, but republication/redistribution requires IEEE permission.
See http://www.ieee.org/publications_standards/publications/rights/index.html for more information.

array processing, which can simultaneously solve the detection and estimation problems. Based on the adaptive rotation of an initial subspace, the adaptive signals parameter estimation and classification technique (ASPECT) algorithm [14] was proposed for removing spurious peaks and obtaining the actual DOAs. The Pisarenko algorithm in combination with the ASPECT principle was used in [15] to develop a new DOA estimation technique without estimating the number of signals. For the case of fully correlated sources, Park *et al.* [16] developed a new algorithm by combining the advantage of WSF for DOA estimation with the ASPECT principle. For reducing the computational complexity, Reddy *et al.* [17] proposed a novel technique that provides a resolution capability comparable with that of the super-resolution techniques. By using the LP model, a new mean-square-error based regularization approach (LP-NMSE) [18] is developed for estimating the DOAs of narrowband signals by introducing multiple regularization parameters into the corrected least squares (CLS) estimation. In the impulsive noise environment, a robust DOA estimator in [19] is proposed by adopting the correntropy as the robust statistics.

Meanwhile, in the conventional array parameter estimation, most algorithms are all based on the array model of narrowband signals, and cannot be applied to DOA estimation for wideband signals. In practice, the assumption of narrowband signals is only approximate, especially when a signal has a significant bandwidth. Based on the theoretical result in [18], we investigate the problem of estimating the DOA of wideband signals with an unknown number of sources in the impulsive noise environment. To suppress the impulsive noise and all other co-channel interferences with different cyclic frequencies, we use a cyclic correntropy function (CCF), which is a generalization of the cyclic autocorrelation function (CAF) for the DOA and the number of sources estimation. First, we propose a theorem of the CCF about phase shift characteristic, and build a linear prediction (LP) model of the CCF from the array data base on the theorem. The DOA of the signals of interest (SOIs) can be estimated by solving the LP coefficients. To achieve a high accuracy of the LP coefficients' estimation, the error caused by the CCF estimation in the limited snapshots regime and the unknown number of SOIs needs to first be obtained. For estimating the estimation error and the number of SOIs only with the accessible data, we use multiple regularization parameters in [18] to stabilize the CLS estimation. By maximizing the maximum correntropy criterion (MCC) of the estimated LP coefficients, we obtain the optimal regularization parameters. Next, an iterative algorithm is proposed to estimate the regularization parameters, variance of the estimation error, and LP coefficients with only a knowledge of the cycle frequency of the SOIs. Finally, the DOA and the number of SOIs are jointly estimated using the results of the iterative algorithm.

The rest of the paper is organized as follows: Section II introduces the CCF and the data model. In Section III, the LP model of the CCF from the array data is built, and the DOA estimation algorithms under both infinite and finite snapshots are given. In Section IV, the MCC-based iterative approach to joint DOA and the number of SOIs estimation is derived, and the main algorithm steps are described. The simulation results and discussions are given in Section V, followed by a concluding summary in Section VI.

II. CYCLIC CORRENTROPY FUNCTION AND DATA MODE

A. CYCLIC CORRENTROPY FUNCTION

The CCF is a generalization of the CAF with information regarding the second and higher-order cyclostationary moments. Compared with the CAF, the CCF has different properties, which can be very useful in non-Gaussian signal processing, especially in the impulsive noise environment [20].

Let $v_x(t,\tau)$ denote the correntropy for a non-stationary process $x(t)$ with time shift τ, which is

$$v_x(t,\tau) = E\left[\kappa\left(x\left(t+\tau/2\right) - x\left(t-\tau/2\right)\right)\right] \tag{1}$$

where $\kappa(\cdot)$ corresponds to any positive-definite symmetric function [21]. In this paper, we employ a Gaussian kernel defined as

$$\kappa(\cdot) = \frac{1}{\sqrt{2\pi}\rho}\exp\left\{-\frac{(\cdot)^2}{2\rho^2}\right\} \tag{2}$$

where ρ is the kernel size. The CCF is characterized by the property that its correntropy $v_x(t,\tau)$ accepts a Fourier transform with respect to time t as follows

$$\begin{aligned} v_x(\varepsilon,\tau) &= \lim_{T\to\infty}\frac{1}{T}\int_{-T/2}^{T/2} v_x(t,\tau)\, e^{-j2\pi\varepsilon t}dt \\ &= \left\langle \kappa\left(x\left(t+\tau/2\right) - x\left(t-\tau/2\right)\right) e^{-j2\pi\varepsilon t}\right\rangle_t \end{aligned} \tag{3}$$

where ε is the cyclic frequency of $x(t)$, and the operator $\langle\cdot\rangle_t$ defines the time averaging operation

$$\langle\cdot\rangle_t = \lim_{T\to\infty}\frac{1}{2T}\int_{-T}^{T}(\cdot)dt \tag{4}$$

Considering a given number of snapshots N, the received signal $x(t)$ can be represented by the discrete-time forms as $x(n)$, and its cyclic correntropy [22] is given as follows

$$\begin{aligned} \hat{v}_x^{(T)}(\varepsilon,\tau) &\triangleq \frac{1}{N}\sum_{n=1}^{N} v_x(n,\tau)\, e^{-j2\pi\varepsilon n} \\ &= \frac{1}{N}\sum_{n=1}^{N}\kappa\left(x\left(n+\tau/2\right) - x\left(n-\tau/2\right)\right) e^{-j2\pi\varepsilon n} \end{aligned} \tag{5}$$

The cyclic correntropy estimator in (5) is asymptotically unbiased and consistent that can be derived following the same lines that are used for the cycle correlation function [20], [23].

B. GENERAL DATA MODEL AND PROBLEM STATEMENT

Consider K independent far-field cyclostationary wideband sources $x_k(t), k \in \{1,\cdots,K\}$ impinging on a uniform linear array (ULA) composed of M identical omni-directional

sensors with inter-element spacings D. We assume that K sources are mutually cyclically uncorrelated and $K_\varepsilon \leq K$ sources corresponding to one cyclic frequency ε. As each array element is isotropic and not affected by the channel inconsistency, mutual coupling and other factors, the data received by the array at the time instant t can be expressed as

$$\mathbf{y}(t) = [y_1(t), y_2(t), \cdots, y_M(t)]^{\mathrm{T}} \tag{6}$$

$$y_m(t) = \sum_{k=1}^{K} x_k(t + \upsilon_{mk}) + n_m(t), \quad m = 1, 2, \cdots, M \tag{7}$$

where $\upsilon_{mk} = (m-1) D \sin\theta_k / c$ is the time delay with respect to the reference antenna, c is the speed of light, θ_k is the DOA of the kth signal, and $n_m(\cdot)$ is the impulsive noise at the mth sensor, which is independent of all signals. Compared with Gaussian noise, the probability density function (PDF) of the impulse noise has a sharper peak and a thicker tail. We propose to use an α-stable distribution [24] to model the measurement noise. Its characteristic function expression is as follows

$$\varphi(t) = \exp(j\mu t - \delta |t|^{\alpha} [1 + j\zeta\, sgn(t)\, \omega(t, \alpha)]) \tag{8}$$

where

$$\omega(t, \alpha) = \begin{cases} \tan\dfrac{\alpha\pi}{2} & \alpha \neq 1 \\ \dfrac{2}{\pi}\log|t| & \alpha = 1 \end{cases}$$

and α $(0 < \alpha \leq 2)$ is the characteristic exponent; δ $(\delta > 0)$ is the dispersion parameter, similar to the concept of variance in the Gaussian distribution; μ $(-\infty < \mu < +\infty)$ is the location parameter; and ζ $(-1 \leq \zeta \leq 1)$ is the index of symmetry. The characteristic exponent α controls the thickness of the density function's tails. When $\alpha = 2$, the α-stable distribution reduces to a Gaussian distribution, and when $\alpha = 1$, it becomes a Cauchy distribution.

For the purposes of this paper, we will address the class of symmetric α-stable (SαS) distributions with $\mu = 0$. A univariate SαS probability density function (pdf) is given by taking the inverse Fourier transform of its characteristic function as follows

$$f(v; \alpha, \delta, \mu)\, \varphi(t) = \frac{1}{2\pi}\int_{-\infty}^{\infty} \exp(\mathrm{j}\mu t - \delta |t|^{\alpha}) e^{-\mathrm{j}tv} dt \tag{9}$$

For illustration purposes, we show in Fig. 1 plots of the SαS pdfs for location parameter $\mu = 0$, dispersion $\delta = 1$, and characteristic exponents $\alpha = 0.5, 1.0, 1.5, 2$. From Fig. 1 we can see that non-Gaussian SαS pdfs ($\alpha = 0.5, 1.0, 1.5$) have much sharper peaks and much heavier tails than the Gaussian pdf ($\alpha = 2$). And the smaller the value of α is, the thicker the tails will be.

Meanwhile, to determine the relative strength of the signal $x(t)$ and impulse noise, the concept of a generalized-signal-to-noise-ratio (GSNR) is defined as [25]

$$\mathrm{GSNR} = 10\log(E\left(|x(t)|^2\right)/\delta) \tag{10}$$

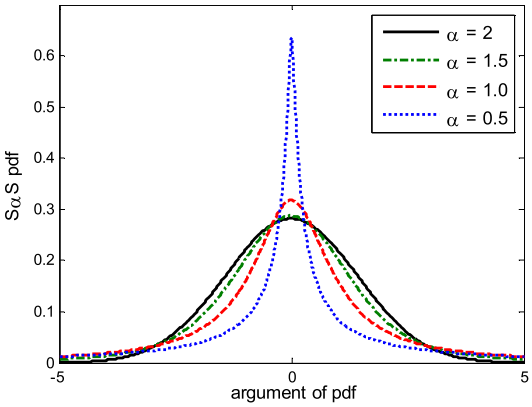

FIGURE 1. *SαS* pdfs of zero location parameter, unit dispersion, and various characteristic exponents α.

C. NARROW-BAND DATA MODEL

If all of the signals $x_k(t)$ are of a narrow band type with the same center frequency f_0, the model in (7) can be approximated as follows

$$y_m(t) \triangleq \sum_{k=1}^{K} x_k(t) \exp(j2\pi f_0 \upsilon_{mk}) + n_m(t) \tag{11}$$

for $m = 1, 2, \cdots, M$.

Many algorithms, such as MUSIC [2], ESPRIT [26] and sparse representation-based DOA estimation methods [27], [28] have been proposed to estimate the DOAs by this narrow-band array mode. However, the model is exact only when the signals are coherent sinusoidal waveforms [29].

III. CLS-BASED CYCLIC CORRENTROPY DOA ESTIMATION

A. LP MODEL OF THE CYCLIC CORRENTROPY FUNCTION OF SENSOR OUTPUTS

First, we propose a simple but important property of the CCF.

Theorem 1: If $x(\cdot)$ is a cyclostationary process with the CCF $v_x(\varepsilon, \tau)$, and $y(t) = x(t + T_0)$, then $v_y(\varepsilon, \tau) = v_x(\varepsilon, \tau) e^{j2\pi\varepsilon T_0}$.

Proof:

$$\begin{aligned} v_y(\varepsilon, \tau) &= \left\langle \kappa\left(y(t+\tau/2) - y(t-\tau/2)\right) e^{-j2\pi\varepsilon t} \right\rangle_t \\ &= \left\langle \kappa\left(x(t+\tau/2+T_0) - x(t-\tau/2+T_0)\right) e^{-j2\pi\varepsilon t} \right\rangle_t \end{aligned} \tag{12}$$

If we consider $t' = t + T_0$, then relation (12) can be expressed as follows

$$\begin{aligned} v_y(\varepsilon, \tau) &= \left\langle \kappa\left(x\left(t'+\tau/2\right) - x\left(t'-\tau/2\right)\right) e^{-j2\pi\varepsilon t'} e^{j2\pi\varepsilon T_0} \right\rangle_{t'} \\ &= v_x(\varepsilon, \tau) e^{j2\pi\varepsilon T_0} \end{aligned} \tag{13}$$

Remark: The point is that the time delay in the signal is transformed into the phase shift of the CCF.

Then, we propose a new method to estimate the parameters for either narrow-band or broad-band signals by using the

LP model of the CCF of the signal outputs. The specific algorithms are as follows:

From (7), we can see that the signals received at different sensors are time delayed versions of one another. So, based on the array model in [18], we first predict the Mth received signal from the other $M-i\,(i=1,\cdots,M-1)$ sensors as follows

$$y_M(t)=\sum_{i=1}^{M-1} y_{M-i}(t+\beta_i)+e_M(t) \tag{14}$$

where β_i are the time delay coefficients that need to be solved, and $e_M(t)$ is the prediction error. By substituting (14) into (3) and using Theorem 1, the CCF of the received signal $y_M(t)$ with a known cycle frequency ε can be predicted from a linear combination of the CCF of the received data from the other $M-1$ sensors as follows

$$\begin{aligned} v^{\varepsilon}_{y_M}(\tau) &= \left\langle \sum_{i=1}^{M-1} \kappa\left[y_{M-i}(t+\tau/2+\beta_i)\right.\right. \\ &\quad \left.\left. -\, y_{M-i}(t-\tau/2+\beta_i)\right] e^{-j2\pi\varepsilon t}\right\rangle_t \\ &= \sum_{i=1}^{M-1} v^{\varepsilon}_{y_{M-i}}(\tau)\, e^{j2\pi\varepsilon\beta_i} \end{aligned} \tag{15}$$

which can be seen as the LP model of the CCF of the sensor outputs. In (15), the terms of the prediction error $e_M(t)$ in (14) disappear because its cyclic correntropy function is always zero when $\varepsilon\neq 0$ [28], [29], therefore by selecting an appropriate cycle frequency ε, the influence of $e_M(t)$ can be reduced. Further, we can rewrite (15) as

$$v^{\varepsilon}_{y_M}(\tau)=\left(\boldsymbol{\varphi}^{\varepsilon}_{y_{M-i}}(\tau)\right)^{\mathrm{T}}\mathbf{q} \tag{16}$$

where

$$\mathbf{q}=\left[e^{j2\pi\varepsilon\beta_1}, e^{j2\pi\varepsilon\beta_2},\cdots, e^{j2\pi\varepsilon\beta_{M-1}}\right]^{\mathrm{T}}\in\mathbb{C}^{(M-1)\times 1},$$

$$\boldsymbol{\varphi}^{\varepsilon}_{y_{M-i}}(\tau)=\left[v^{\varepsilon}_{y_{M-1}}(\tau), v^{\varepsilon}_{y_{M-2}}(\tau),\cdots, v^{\varepsilon}_{y_1}(\tau)\right]^{\mathrm{T}}\in\mathbb{C}^{(M-1)\times 1}.$$

Suppose that we observe $\mathbf{y}(t)$ from the array data $\{y_1(t), y_2(t),\cdots, y_M(t)\}_{t=0}^{N-1}$. Then, setting the lag τ to be $\tau=0,1,\cdots,N$ yields the compact vector-matrix form of the LP model (16) as follows

$$\mathbf{v}=\boldsymbol{\Phi}\mathbf{q} \tag{17}$$

where

$$\mathbf{v}=\left[v^{\varepsilon}_{y_M}(0), v^{\varepsilon}_{y_M}(1),\cdots, v^{\varepsilon}_{y_M}(N-1)\right]^{\mathrm{T}}\in\mathbb{C}^{N\times 1},$$

$$\boldsymbol{\Phi}=\left[\boldsymbol{\varphi}^{\varepsilon}_{y_{M-i}}(0), \boldsymbol{\varphi}^{\varepsilon}_{y_{M-i}}(1),\cdots, \boldsymbol{\varphi}^{\varepsilon}_{y_{M-i}}(N-1)\right]^{\mathrm{T}}\in\mathbb{C}^{N\times(M-1)}.$$

B. DOA ESTIMATION UNDER INFINITE SNAPSHOT

We can see that the DOA of the SOIs can be estimated from the LP model parameter $\boldsymbol{q}$. The minimum LS estimate $\mathbf{q}$ can be obtained from

$$\mathbf{q}=\left(\boldsymbol{\Phi}^{\mathrm{H}}\boldsymbol{\Phi}\right)^{-1}\boldsymbol{\eta} \tag{18}$$

where $\boldsymbol{\eta}=\boldsymbol{\Phi}^{\mathrm{H}}\mathbf{v}$ of length $M-1$. Another method to solve $\mathbf{q}$ is to use the eigenvalue decomposition (EVD) of the matrix $\boldsymbol{\Sigma}=\boldsymbol{\Phi}^{\mathrm{H}}\boldsymbol{\Phi}$.

$$\boldsymbol{\Sigma}=\boldsymbol{\Phi}^{\mathrm{H}}\boldsymbol{\Phi}=\mathbf{U}\boldsymbol{\Lambda}\mathbf{U}^{\mathrm{H}} \tag{19}$$

where $\mathbf{U}=[\mathbf{u}_1,\mathbf{u}_2,\cdots,\mathbf{u}_{M-1}]$, $\mathbf{U}\mathbf{U}^{\mathrm{H}}=\mathbf{U}^{\mathrm{H}}\mathbf{U}=\mathbf{I}_{M-1}$, and $\boldsymbol{\Lambda}=\mathrm{diag}\,(\lambda_1,\lambda_2,\cdots,\lambda_{M-1})$, where $\{\mathbf{u}_i\}_{i=1}^{M-1}$ and $\{\lambda_i\}_{i=1}^{M-1}$ are the corresponding eigenvectors and eigenvalues, respectively.

Lemma: When the number of snapshots converges to infinity, the number of the signals of interest (SOIs) with cycle frequency α is equal to the rank of the matrix $\boldsymbol{\Sigma}$.

Proof: See Appendix A

Accordingly, when N tends to infinity, we obtain $\lambda_1\geq\lambda_2\geq\cdots\geq\lambda_{K_\varepsilon}\geq\lambda_{K_\varepsilon+1}=\cdots=\lambda_{M-1}=0$. Next, the coefficient $\mathbf{q}$ in (17) is given by

$$\mathbf{q}=\sum_{i=1}^{M-1}\frac{\mathbf{u}_i\mathbf{u}_i^{\mathrm{H}}}{\lambda_i}\boldsymbol{\eta}=\sum_{i=1}^{K_\varepsilon}\frac{\mathbf{u}_i\mathbf{u}_i^{\mathrm{H}}}{\lambda_i}\boldsymbol{\eta} \tag{20}$$

From the LP model parameters $\mathbf{q}=\left\{e^{j2\pi\varepsilon\beta_i}\right\}_{i=1}^{M-1}$, the DOA of the SOIs can be estimated by searching for the positions of the peaks of a prediction polynomial as follows

$$P(\theta)=\frac{1}{\left|1-e^{j2\pi\varepsilon\beta_1}w^{-1}-\cdots-e^{j2\pi\varepsilon\beta_{M-1}}w^{-M-1}\right|^2} \tag{21}$$

where $w=e^{j2\pi\varepsilon D\sin\theta/c}$.

C. DOA ESTIMATION BY THE CORRECTED LEAST-SQUARES METHOD

In practice, the CCF has to be estimated from a finite sample of the received signal that caused estimation error as follows:

$$\hat{v}^{\varepsilon}_{y_i}(\tau)=v^{\varepsilon}_{y_i}(\tau)+\Delta v^{\varepsilon}_{y_i}(\tau),\quad i=1,\cdots,M-1 \tag{22}$$

where $\Delta v^{\varepsilon}_{y_i}(\tau)$ is the estimation error. By substituting (22) into (16), we obtain

$$\begin{aligned} \hat{v}^{\varepsilon}_{y_M}(\tau) &= \left(\hat{\boldsymbol{\varphi}}^{\varepsilon}_{y_{M-i}}(\tau)-\boldsymbol{\Delta\varphi}^{\varepsilon}_{y_{M-i}}(\tau)\right)^{\mathrm{T}}\mathbf{q}+\Delta v^{\varepsilon}_{y_M}(\tau) \\ &= \hat{\boldsymbol{\varphi}}^{\varepsilon}_{y_{M-i}}(\tau)\,\mathbf{q}+e(\tau) \end{aligned} \tag{23}$$

where

$$\hat{\boldsymbol{\varphi}}^{\varepsilon}_{y_{M-i}}(\tau)=\left[\hat{v}^{\varepsilon}_{y_{M-1}}(\tau), \hat{v}^{\varepsilon}_{y_{M-2}}(\tau),\cdots, \hat{v}^{\varepsilon}_{y_1}(\tau)\right]^{\mathrm{T}}\in\mathbb{C}^{(M-1)\times 1},$$

$$\boldsymbol{\Delta\varphi}^{\varepsilon}_{y_{M-i}}(\tau)=\left[\Delta\varphi^{\varepsilon}_{y_{M-1}}(\tau), \Delta\varphi^{\varepsilon}_{y_{M-2}}(\tau),\cdots, \Delta\varphi^{\varepsilon}_{y_1}(\tau)\right]^{\mathrm{T}}\in\mathbb{C}^{(M-1)\times 1}$$

$$e(\tau)=\Delta v^{\varepsilon}_{y_M}(\tau)-\left(\Delta\varphi^{\varepsilon}_{y_{M-i}}(\tau)\right)^{\mathrm{T}}\mathbf{q}=\boldsymbol{\Delta\psi}^{\varepsilon}_{y_{M-i}}(\tau)\,\mathbf{w},$$

$$\mathbf{w}=(1,-\mathbf{q})^{T},$$

$$\boldsymbol{\Delta\psi}^{\varepsilon}_{y_{M-i}}(\tau)=\left(\hat{v}^{\varepsilon}_{y_M}(\tau), \hat{\boldsymbol{\varphi}}^{\varepsilon}_{y_{M-i}}(\tau)\right)^{\mathrm{T}}.$$

Next, we use the multiple lags $\tau=0,1,\cdots,N-1$ for a new vector form as follows

$$\hat{\mathbf{v}}=\hat{\boldsymbol{\Phi}}\mathbf{q}+\mathbf{e} \tag{24}$$

where

$$\hat{\mathbf{v}} = \left[\hat{v}^{\varepsilon}_{y_M}(0), \hat{v}^{\varepsilon}_{y_M}(1), \cdots, \hat{v}^{\varepsilon}_{y_M}(N-1)\right]^{\mathrm{T}} \in \mathbb{C}^{N\times 1},$$

$$\hat{\mathbf{\Phi}} = \left[\hat{\boldsymbol{\varphi}}^{\varepsilon}_{y_{M-i}}(0), \hat{\boldsymbol{\varphi}}^{\varepsilon}_{y_{M-i}}(1), \cdots, \hat{\boldsymbol{\varphi}}^{\varepsilon}_{y_{M-i}}(N-1)\right]^{\mathrm{T}} \in \mathbb{C}^{N\times(M-1)},$$

$$\mathbf{e} = [e(0), e(1), \cdots, e(N-1)]^{\mathrm{T}} = \mathbf{\Delta\Psi} w \in \mathbb{C}^{N\times 1},$$

$$\mathbf{\Delta\Psi} = \left[\mathbf{\Delta}\boldsymbol{\psi}^{\varepsilon}_{y_{M-i}}(1), \mathbf{\Delta}\boldsymbol{\psi}^{\varepsilon}_{y_{M-i}}(2)\cdots, \mathbf{\Delta}\boldsymbol{\psi}^{\varepsilon}_{y_{M-i}}(N-1)\right]^{\mathrm{T}} \in \mathbb{C}^{N\times(M-1)}.$$

Due to the estimation error $\mathbf{e}$, the LS estimation of $\mathbf{q}$ in (24) is not consistent and unbiased [30]. For simplicity, we assume $\mathbf{e}$ is an asymptotic normal distribution with a zero mean and a variance estimated as

$$\sigma^2 = \left\|\hat{\mathbf{v}} - \hat{\mathbf{\Phi}}\mathbf{q}\right\|^2 \tag{25}$$

From (24), the CLS estimation of the parameter $\mathbf{q}$ is given by

$$\hat{\mathbf{q}}_{\sigma^2} = \left(\hat{\mathbf{\Phi}}^{\mathrm{H}}\hat{\mathbf{\Phi}} - \sigma^2\mathbf{I}_{M-1}\right)^{-1}\hat{\boldsymbol{\eta}} \tag{26}$$

where $\hat{\boldsymbol{\eta}} = \hat{\mathbf{\Phi}}^{\mathrm{H}}\hat{\mathbf{v}}$. As in (20), we can also implement the EVD of $\hat{\mathbf{\Sigma}} = \hat{\mathbf{\Phi}}^{\mathrm{H}}\hat{\mathbf{\Phi}}$ to derive

$$\hat{\mathbf{q}}_{\sigma^2} = \sum_{i=1}^{M-1}\frac{\hat{\mathbf{u}}_i\hat{\mathbf{u}}_i^{\mathrm{H}}}{\hat{\lambda}_i - \sigma^2}\hat{\boldsymbol{\eta}} \tag{27}$$

where $\{\hat{\mathbf{u}}_i\}$ and $\{\hat{\lambda}_i\}$ are the eigenvectors and eigenvalues of the matrix $\mathbf{\Sigma} = \hat{\mathbf{\Phi}}^{\mathrm{H}}\hat{\mathbf{\Phi}}$, respectively.

IV. MCC-BASED ITERATIVE APPROACH TO JOINT DOA AND NUMBER OF SIGNALS ESTIMATION

A. MAXIMUM CORRENTROPY CRITERION ESTIMATION

In this section, we estimate the number of the SOIs by introducing a regularization matrix $\mathbf{P}$ [18] that also stabilizes the CLS estimation into (26) expressed by

$$\hat{\mathbf{q}}_{\sigma^2,p} = \left(\hat{\mathbf{\Phi}}^{\mathrm{H}}\hat{\mathbf{\Phi}} - \sigma^2\mathbf{I}_{m-1} + \mathbf{P}\right)^{-1}\hat{\boldsymbol{\eta}} \tag{28}$$

The EVD of the matrix $\mathbf{P}$ is shown as follows

$$\begin{aligned}\mathbf{P} &= \mathbf{V}\mathbf{R}\mathbf{V}^{\mathrm{H}}\\ \mathbf{R} &= \mathrm{diag}(\gamma_1, \gamma_2, \cdots, \gamma_{M-1})\end{aligned} \tag{29}$$

where $\{\gamma_i\}$ are the regularization parameters. Next, we can rewrite (28) as follows

$$\hat{\mathbf{q}}_{\sigma^2,p}(\{\gamma_i\}) = \sum_{i=1}^{M-1}\frac{\hat{\mathbf{u}}_i\hat{\mathbf{u}}_i^{H}}{\hat{\lambda}_i - \sigma^2 + \gamma_i}\hat{\boldsymbol{\eta}} \tag{30}$$

where $\hat{\boldsymbol{\eta}} = \hat{\mathbf{\Phi}}^{\mathrm{H}}\hat{\mathbf{v}}$.

Judging from the above, it is easy to show that the rank of $\hat{\mathbf{\Phi}}^{\mathrm{H}}\hat{\mathbf{\Phi}} - \sigma^2\mathbf{I}_{m-1}$ approximates to K_ε, where K_ε is the number of the SOIs. Therefore, our objective for introducing the parameters $\{\gamma_i\}$ is to retain K_ε eigenvalues $\hat{\lambda}_i$, $i = 1, 2, \cdots, K_\varepsilon$, and further reduce the effect of the other eigenvalues $\hat{\lambda}_i$, $i = K_\varepsilon+1, \cdots, M-1$. To this end, the parameters $\{\gamma_i\}$ should satisfy the following equation

$$\gamma_i = \begin{cases}0, & \text{for} i = 1, \cdots, K_\varepsilon\\ \infty, & \text{for} i = K_\varepsilon + 1, \cdots, M-1\end{cases} \tag{31}$$

Next, the problem becomes how to confirm the parameters $\{\gamma_i\}$ to meet the above conditions in (31). As the MCC proposed in [31] and [32] is applicable in any noise environment whose distribution has the maximum at the origin and outperforms the mean square error (MSE) in the case of impulsive noise, we consider the MCC of the estimate $\hat{\mathbf{q}}_{\sigma^2,p}$ in (28) defined by

$$\mathrm{MCC} = E\left[\kappa\left(\mathbf{q} - \hat{\mathbf{q}}_{\sigma^2,p}\right)\right] \tag{32}$$

Theorem 2: The asymptotic MCC of the estimated $\hat{\mathbf{q}}_{\sigma^2,p}(\{\gamma_i\})$ in (30) is given as the following function of $\{\gamma_i\}$, provided that N is sufficiently large.

$$\mathrm{MCC}(\{\gamma_i\}) = \frac{1}{\sqrt{2\pi}\rho}\sum_{i=1}^{M-1}\exp\left\{-\frac{\sigma^2\hat{\lambda}_i\left(1+\|\mathbf{q}\|^2\right)}{2\rho^2 N\left(\hat{\lambda}_i - \sigma^2 + \gamma_i\right)^2} - \frac{\sigma^4\left|\hat{\mathbf{u}}_i^{\mathrm{H}}\mathbf{q}\right|^2 + N\gamma_i^2\left|\hat{\mathbf{u}}_i^{\mathrm{H}}\mathbf{q}\right|^2}{2\rho^2 N\left(\hat{\lambda}_i - \sigma^2 + \gamma_i\right)^2}\right\} \tag{33}$$

Proof: See Appendix B.

Next, we can obtain an accurate estimate of $\hat{\mathbf{q}}_{\sigma^2,p}(\{\gamma_i\})$ with a maximum MCC. The ith terms related to γ_i in (33) are picked as follows

$$\mathrm{MCC}(\gamma_i) = \frac{1}{\sqrt{2\pi}\rho}\exp\left\{-\frac{\sigma^2\hat{\lambda}_i\left(1+\|\mathbf{q}\|^2\right)}{2\rho^2 N\left(\hat{\lambda}_i - \sigma^2 + \gamma_i\right)^2} - \frac{\sigma^4\left|\hat{\mathbf{u}}_i^{\mathrm{H}}\mathbf{q}\right|^2 + N\gamma_i^2\left|\hat{\mathbf{u}}_i^{\mathrm{H}}\mathbf{q}\right|^2}{2\rho^2 N\left(\hat{\lambda}_i - \sigma^2 + \gamma_i\right)^2}\right\} \tag{34}$$

For $\gamma_i = 0$ and $\gamma_i = \infty$, we obtain

$$\begin{cases}\mathrm{MCC}(\gamma_i = 0) = \dfrac{1}{\sqrt{2\pi}\rho} \times \exp\left\{-\dfrac{\sigma^2\hat{\lambda}_i\left(1+\|\mathbf{q}\|^2\right) + \sigma^4\left|\hat{\mathbf{u}}_i^{\mathrm{H}}\mathbf{q}\right|^2}{2\rho^2 N\left(\hat{\lambda}_i - \sigma^2\right)^2}\right\}\\ \mathrm{MCC}(\gamma_i = \infty) = \dfrac{1}{\sqrt{2\pi}\rho}\exp\left\{-\dfrac{\left|\hat{\mathbf{u}}_i^{\mathrm{H}}\mathbf{q}\right|^2}{2\rho^2}\right\}\end{cases} \tag{35}$$

If $\gamma_i = 0$ is adopted, then

$$\mathrm{MCC}(\gamma_i = 0) \geq \mathrm{MCC}(\gamma_i = \infty) \tag{36}$$

By substituting (35) into (36), we obtain

$$\frac{\sigma^2\hat{\lambda}_i\left(1+\|\mathbf{q}\|^2\right) + \sigma^4\left|\hat{\mathbf{u}}_i^{\mathrm{H}}\mathbf{q}\right|^2}{2\rho^2 N\left(\hat{\lambda}_i - \sigma^2\right)^2} \leq \frac{\left|\hat{\mathbf{u}}_i^{\mathrm{H}}\mathbf{q}\right|^2}{2\rho^2} \tag{37}$$

Rewrite (37) as follows

$$\hat{\lambda}_i - \sigma^2 \geq \frac{\sigma^2 \lambda_i \left(1 + \|\mathbf{q}\|^2\right)}{N \left|\hat{\mathbf{u}}_i^{\mathrm{H}} \mathbf{q}\right|^2 \left(\hat{\lambda}_i - \sigma^2\right)} + \frac{\sigma^4}{N \left(\hat{\lambda}_i - \sigma^2\right)} \tag{38}$$

So that γ_i in (31) can be obtained as

$$\gamma_i = \begin{cases} 0 & \hat{\lambda}_i - \sigma^2 \geq \gamma_i^* \\ \infty & \hat{\lambda}_i - \sigma^2 < \gamma_i^* \end{cases} \tag{39}$$

where γ_i^* is the optimal regularization parameter defined as

$$\gamma_i^* = \frac{\sigma^2 \hat{\lambda}_i \left(1 + \|\mathbf{q}\|^2\right)}{N \left|\hat{\mathbf{u}}_i^{\mathrm{H}} \mathbf{q}\right|^2 \left(\hat{\lambda}_i - \sigma^2\right)} + \frac{\sigma^4}{N \left(\hat{\lambda}_i - \sigma^2\right)} \tag{40}$$

Comparing (39) with (31), we can see that the number of SOIs can be estimated by determining γ_i^* and comparing $\hat{\lambda}_i - \sigma^2$ to γ_i^*.

B. ITERATIVE ALGORITHM FOR THE ESTIMATION OF THE DOA AND NUMBER OF THE SOIs

To jointly estimate the DOA and the number of SOIs, we solve the unknown parameters $\left\{\gamma_i^*\right\}_{i=1}^{M-1}$ in (40) and $\hat{\mathbf{q}}_{\sigma^2,p}\left(\{\gamma_i\}\right)$ in (30). In the case of $K_\varepsilon < M-1$, $\{\gamma_i\}_{i=1}^{M-1}$ in (38) satisfies the following relationship:

$$\frac{|\gamma_{M-1}|}{|\gamma_1|} > \chi \tag{41}$$

where χ is a specified large value (e.g., $\chi = 10^{50}$). Specifically, the steps of the iterative algorithm are shown as follows:

Step 1 Estimate the cyclic correntropy function for the $M-$ th sensor and the other $M-1$ sensors by the finite-sample N as

$$\hat{v}_{y_m}^a(i) = \left\{ \frac{1}{N} \sum_{n=0}^{N-1-i} \kappa\left(y_m(n+i) - y_m(n)\right) e^{-j\frac{2\pi}{N}an} \right\} e^{-j\frac{\pi}{N}ai}, \quad m = 1, 2, \cdots, M \tag{42}$$

where $a = (\varepsilon/f_s) N \in [0, f_s]$ is the digital cyclic frequency, and the adjustment term $e^{-j\pi/Nai}$ makes the sequence symmetric with respect to a.

For $i = 0, 1, \cdots, N-1$, we have the following cyclic correntropy matrix

$$\hat{\mathbf{v}} = \left[\hat{v}_{y_M}^a(0), \hat{v}_{y_M}^a(1), \cdots, \hat{v}_{y_M}^a(L-1)\right]^{\mathrm{T}} \tag{43}$$

$$\hat{\mathbf{\Phi}} = \begin{bmatrix} v_{y_{M-1}}^a(0) & v_{y_{M-1}}^a(1) & \cdots & v_{y_{M-1}}^a(L-1) \\ v_{y_{M-2}}^a(0) & v_{y_{M-2}}^a(1) & \cdots & v_{y_{M-2}}^a(L-1) \\ \vdots & \vdots & \ddots & \vdots \\ v_{y_1}^a(0) & v_{y_1}^a(1) & \cdots & v_{y_1}^a(L-1) \end{bmatrix}^{\mathrm{T}} \tag{44}$$

Step 2 Calculate the eigenvalues $\left\{\hat{\lambda}_i\right\}_{i=1}^{M-1}$ and the eigenvectors $\left\{\hat{\mathbf{u}}_i\right\}_{i=1}^{M-1}$ of the data matrix $\hat{\mathbf{\Phi}}$ by using the EVD as follows

$$\hat{\mathbf{\Sigma}} = E\left[\hat{\mathbf{\Phi}}^{\mathrm{H}} \hat{\mathbf{\Phi}}\right] = \hat{\mathbf{U}} \hat{\mathbf{\Lambda}} \hat{\mathbf{U}}^{\mathrm{H}} \tag{45}$$

where $\hat{\mathbf{U}} = \left[\hat{\mathbf{u}}_1, \cdots, \hat{\mathbf{u}}_{M-1}\right]$, and $\hat{\mathbf{\Lambda}} = \mathrm{diag}\left(\hat{\lambda}_1, \cdots, \hat{\lambda}_{M-1}\right)$.

Step 3 Set $k = 0$, with the initial values of the variance of the estimation error $\sigma^{2(k)}$ and the regularization parameters $\left\{\gamma_i^{(k)}\right\}_{i=1}^{M-1}$ exceeding a specified value ξ, where ξ is chosen to be a small positive number$\left(e.g., \xi = 10^{-50}\right)$

Step 4 Calculate the estimate $\hat{\mathbf{q}}_{\sigma^{2(k)},p}\left(\left\{\gamma_i^{(k)}\right\}\right)$ in (30) for the given $\sigma^{2(k)}$ and $\left\{\gamma_i^{(k)}\right\}_{i=1}^{M-1}$ as

$$\hat{\mathbf{q}}_{\sigma^{2(k)},p}\left(\left\{\gamma_i^{(k)}\right\}\right) = \sum_{i=1}^{M-1} \frac{\hat{\mathbf{u}}_i \hat{\mathbf{u}}_i^{\mathrm{H}}}{\hat{\lambda}_i - \sigma^{2(k)} + \gamma_i^{(k)}} \hat{\boldsymbol{\eta}} \tag{46}$$

where $\hat{\boldsymbol{\eta}} = \hat{\mathbf{\Phi}}^{\mathrm{H}} \hat{\mathbf{v}}$.

Step 5 Update the optimal regularization parameters $\left\{\gamma_i^{(k+1)}\right\}_{i=1}^{M-1}$ based on (40) with the estimate $\hat{\mathbf{q}}_{\sigma^{2(k)},p}\left(\left\{\gamma_i^{(k)}\right\}\right)$ in Step 4 as

$$\gamma_i^{(k+1)} = \frac{\sigma^2 \hat{\lambda}_i \left(1 + \left\|\hat{\mathbf{q}}_{\sigma^{2(k)},p}\left(\gamma_i^{(k)}\right)\right\|^2\right)}{N \left|\hat{\mathbf{u}}_i^{\mathrm{H}} \hat{\mathbf{q}}_{\sigma^{2(k)},p}\left(\gamma_i^{(k)}\right)\right|^2 \left(\hat{\lambda}_i - \sigma^{2(k)}\right)} + \frac{\sigma^{4(k)}}{N \left(\hat{\lambda}_i - \sigma^{2(k)}\right)} \tag{47}$$

for $i = 1, \cdots, M-1$.

Step 6 Update the variance of the estimation error $\sigma^{2(k+1)}$ based on (25) for the estimate $\hat{\mathbf{q}}_{\sigma^2,p}\left(\left\{\gamma_i^{(k)}\right\}\right)$ in Step 4 as

$$\sigma^{2(k+1)} = \left\|\hat{\mathbf{v}} - \hat{\mathbf{\Phi}} \hat{\mathbf{q}}_{\sigma^{2(k)},p}\left(\left\{\gamma_i^{(k)}\right\}\right)\right\|^2 \tag{48}$$

Step 7 Calculate the ratio ϑ of $\gamma_{M-1}^{(k+1)}$ to $\gamma_1^{(k+1)}$, which is obtained in Step 5 as

$$\vartheta = \frac{\left|\gamma_{M-1}^{(k+1)}\right|}{\left|\gamma_1^{(k+1)}\right|} \tag{49}$$

Set $k = k+1$, and then go back to Step 4 and repeat the iteration. If θ increases over a specified large value χ, the iteration is stopped. The number of the SOIs can be estimated by referring to the relationship between the eigenvalues $\left\{\hat{\lambda}_i - \sigma^2\right\}_{i=1}^{M-1}$ and the regularization parameters $\left\{\gamma_i^{(k+1)}\right\}_{i=1}^{M-1}$ in (47).

From the results, the CLS estimation of the LP parameters $\hat{\mathbf{q}}_{\sigma^2,p}\left(\{\gamma_i\}\right)$ can be obtained via (30), where the parameters $\{\gamma_i\}_{i=1}^{M-1}$ and σ^2 are the iteration results of $\left\{\gamma_i^{(k+1)}\right\}_{i=1}^{M-1}$ and $\sigma^{2(k+1)}$, respectively, or a close result can be derived from the eigenvalues $\left\{\hat{\lambda}_i\right\}_{i=1}^{K_\varepsilon}$ as

$$\hat{\mathbf{q}}_{\sigma^2} = \sum_{i=1}^{K_\varepsilon} \frac{\hat{\mathbf{u}}_i \hat{\mathbf{u}}_i^H}{\hat{\lambda}_i - \sigma^2} \hat{\boldsymbol{\eta}} \tag{50}$$

Finally, the DOA of the SOIs can be estimated from the peak positions of the spectrum $P(\theta)$ in (21).

TABLE 1. Computational complexity of each step.

Step	Addition/subtraction and multipications	Division, matrix inversion, and exponentiation
1	$(M-1)(2LN-L^2-L-N)$	$(M-1)(NL+2N-(L+1)L/2)$
2	$(M-1)(2L-1)$	1
3	0	0
4	$3(M-1)^2$	$M-1$
5	$4(M-1)$	1
6	$2ML-1$	0
7	0	1

According to the steps of the iterative algorithm, we analyze the computational complexity in terms of the floating point operations for the proposed algorithm. The computational complexity of the each step in the iterative algorithm are given in Table 1. Based on Table 1, the order of overall computational complexity of the proposed algorithm is $O(MLN)$.

V. SIMULATIONS

We consider a uniform linear array of $M = 10$ sensors with a half-wavelength spacing. The SOIs are two far-field BPSK signals with a raised cosine pulse shape with one center frequency of 100MHz and 40% excess bandwidth from two different directions. The interference signal is a far-field wideband AM signal with the same center frequency as the SOIs and a relative wideband of 30%. For assessing the detection performance of the estimation of the number of SOIs, the robust minimum description length (RMDL) [33], Akaike information criterion (AIC) [12], and the modified Gerschgorin disk estimator (MGDE) [34] are performed. The measure of the detection of the number of SOIs is the detection probability P, which is defined as the ratio of the number of correct estimates to the number of Monte Carlo experiments.

To examine the estimation performance for estimating the DOA, the cyclic MUSIC [29], the wideband covariance matrix sparse representation (W-CMSR) [35] and the robust covariation-based MUSIC (ROC-MUSIC) [7] are conducted. In the examples of DOA estimation, we assume that the number of SOIs is known. As the W-CMSR and ROC-MUSIC algorithms cannot mitigate co-channel interferences with the same center frequency, the number of sources is assumed to be three, whereas for the cyclic MUSIC and the proposed algorithm, only two SOIs are considered. We perform 200 Monte-Carlo runs in every experiment and compute the resolution event probability and the root-mean-square error (RMSE) of the DOA estimates. The resolution analysis of these algorithms are studied by a resolution criterion defined by the following threshold equation [36]

$$\Lambda\left(\hat{\theta}_1,\hat{\theta}_2\right) \triangleq P\left(\hat{\theta}_m\right) - \frac{1}{2}\left[P\left(\hat{\theta}_1\right)+P\left(\hat{\theta}_2\right)\right] > 0 \quad (51)$$

where $\hat{\theta}_1$ and $\hat{\theta}_2$ are the estimated angles of arrival of the SOIs, and $\hat{\theta}_m = \left(\hat{\theta}_1+\hat{\theta}_2\right)/2$ is the mid-range. In the case of angular resolution, we further analyze the RMSE of the algorithms, that is,

$$\text{RMSE} = \frac{1}{K_\epsilon}\sum_{k=1}^{K_\epsilon}\sqrt{\frac{1}{L}\sum_{l=1}^{L}\left[\widehat{\theta}_k(l)-\theta_k\right]^2} \quad (52)$$

where θ_k and $\widehat{\theta}_k(l)$ are the true and estimated values of the angles of arrival in the l-th experiment, respectively, and L is the total number of successful runs.

A. PERFORMANCE OF DOA AND NUMBER OF SOIs ESTIMATION

In this experiment, we set the number of snapshots $N = 6000$, the generalized SNR GSNR $=$ 8dB, and the characteristic exponent of the noise $\alpha = 1.5$, and the kernel size is set at $\rho = 1.5$. The angles of arrival for the two SOIs are 25° and 50°, respectively, and the AM interference arrives from a direction of 20°.

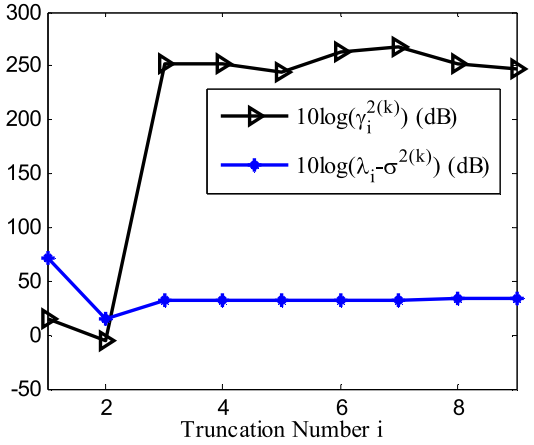

FIGURE 2. Comparison of the estimated eigenvalues $\left\{\hat{\lambda}_i-\sigma^{2(k)}\right\}$ and the regularization parameters $\left\{\gamma_i^{(k)}\right\}$ with $i = 1$ to $M-1$ in the last iteration.

First, we testify the effectiveness of the detection of the number of SOIs. Fig. 2 shows the change of $\left\{\gamma_i^{(k)}\right\}$ and $\hat{\lambda}_i-\sigma^{2(k)}$ with $i = 1$ to $M-1$ in the last iteration. We found that the number of SOIs is determined by the intersection of these two curves $\hat{K}_\varepsilon = i = 2$. It becomes clear that the $\left\{\gamma_i^{(k)}\right\}$ and $\sigma^{2(k)}$ obtained from the proposed iterative algorithm in the 2nd subsection of Sec IV are essential for estimating the number of SOIs. Furthermore, in order to verify the estimated accuracy of the parameters $\left\{\gamma_i^{(k)}\right\}$, we show the case of divergence and convergence of $\left\{\gamma_i^{(k)}\right\}$ with respect to k iterations and the theoretically optimal regularization parameter $\left\{\gamma_i^*\right\}$ for reference in Fig. 3. In addition, the theoretical parameter $\left\{\gamma_i^*\right\}$ is calculated using (40), where the theoretical LP parameter $\mathbf{q}$ can be obtained in (20) with the simulation condition $K_\varepsilon = 2$, and the theoretical variance σ^2 can be given in (25) with the theoretical parameter $\mathbf{q}$ and the true matrix $\mathbf{\Phi}$ in (17). As expected, the estimated parameters

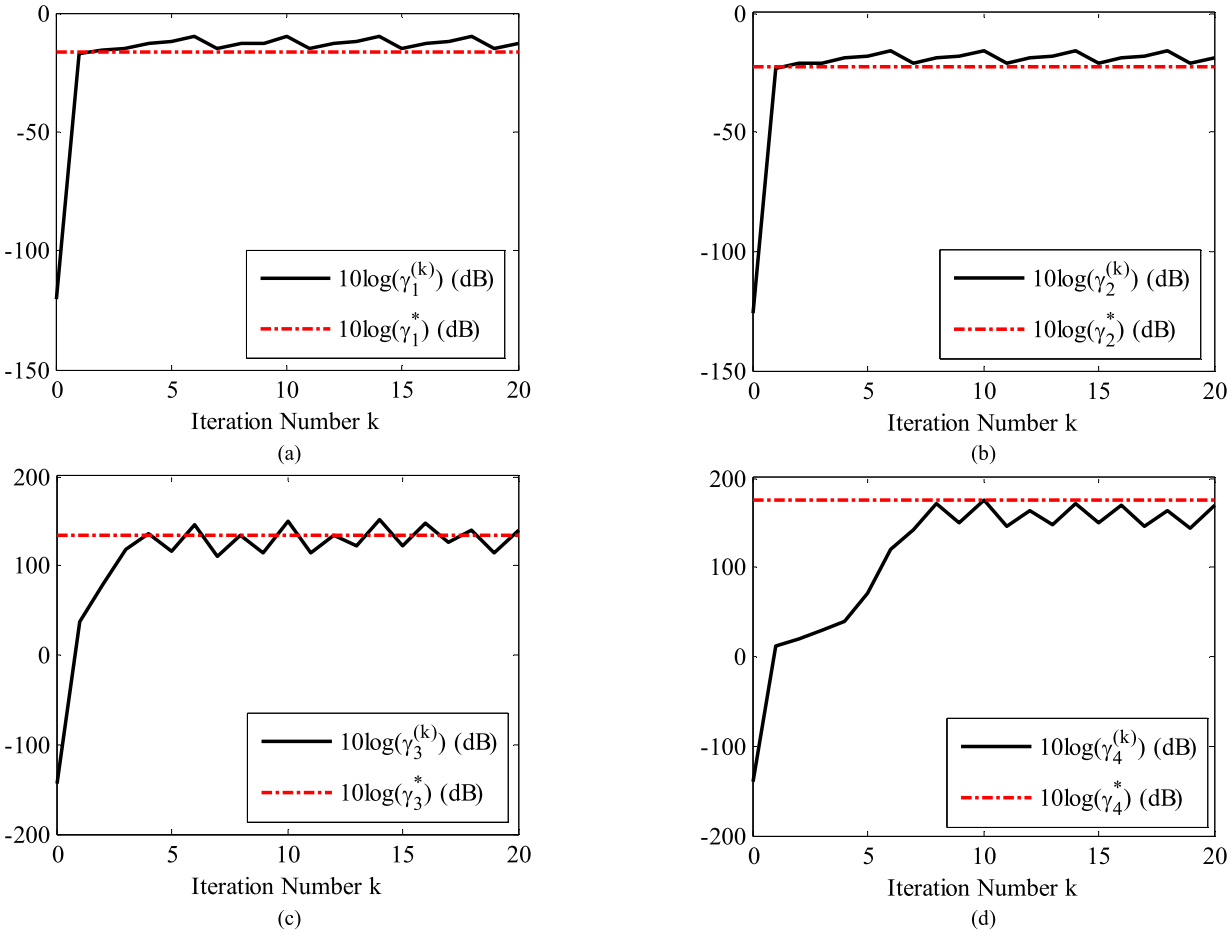

FIGURE 3. Profiles of the regularization parameters $\gamma_1^{(k)}$ (a), $\gamma_2^{(k)}$ (b), $\gamma_3^{(k)}$ (c), and $\gamma_4^{(k)}$ (d) calculated by the proposed algorithm.

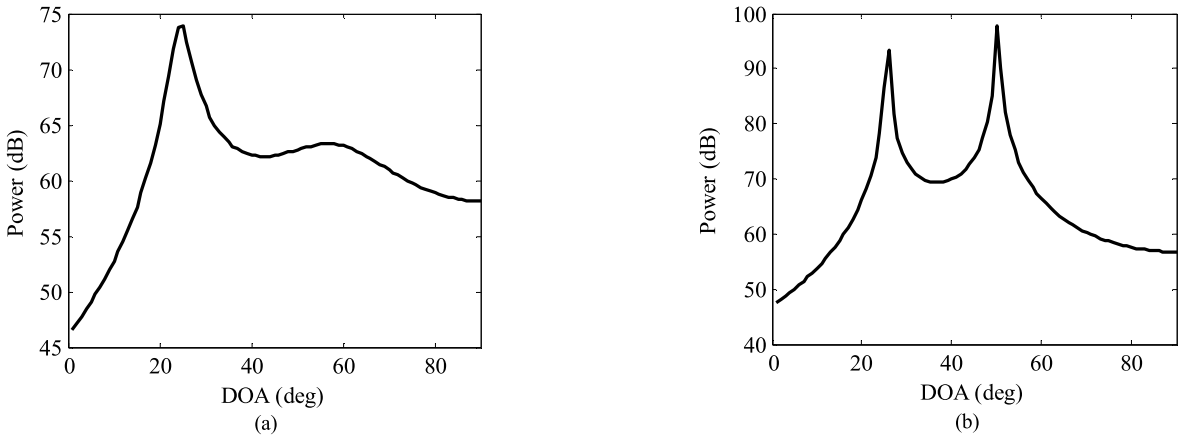

FIGURE 4. DOA of SOIs, which are estimated by the coefficients **q** (a) and the coefficients $\hat{\mathbf{q}}_{\mu^2,p}(\{\gamma_i\})$ (b).

$\gamma_1^{(k)}$ and $\gamma_2^{(k)}$ converge close to zero (e.g., $1e^{-20}$) in a few iterations, whereas $\gamma_3^{(k)}$ and $\gamma_4^{(k)}$ diverge to a very large value (e.g., $1e^{150}$).

Next, we examine the performance of the DOA estimation via the proposed algorithm. Fig. 4 shows the results of the DOA of SOIs, which are estimated with the coefficients **q** in (18) and the coefficients $\hat{\mathbf{q}}_{\sigma^2,p}(\{\gamma_i\})$ in (30). Since the solution to **q** in (18) is directly obtained from LS without considering the influence of the estimation error caused by the finite amount of data, the estimation result is poor. However, we make a more accurate estimate of the parameter $\hat{\mathbf{q}}_{\sigma^2,p}(\{\gamma_i\})$ in (30) by the estimation error σ^2 obtained by the proposed iterative algorithm. From the results we see that the variance of the estimation error σ^2 caused by the

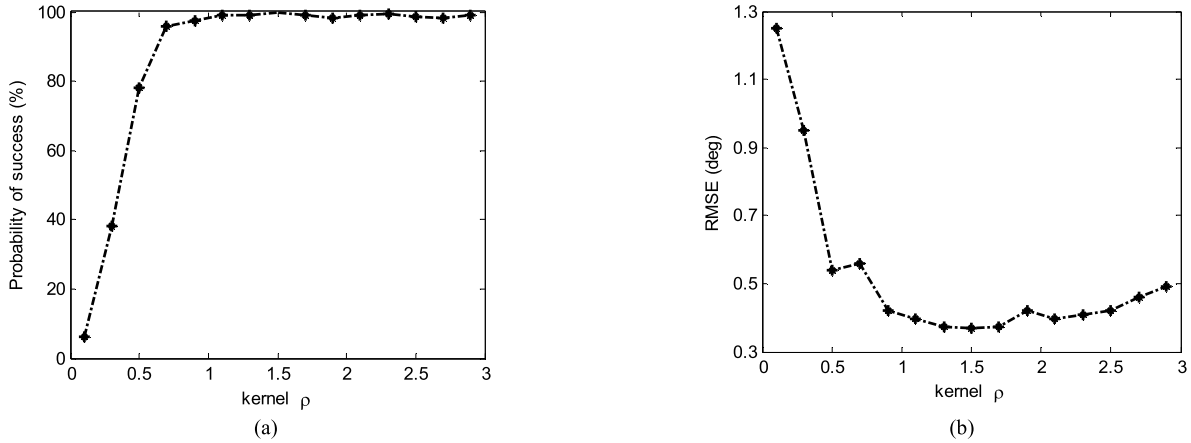

FIGURE 5. Probability of success (a) and RMSE (b) of the TDE estimation as a function of the kernel size.

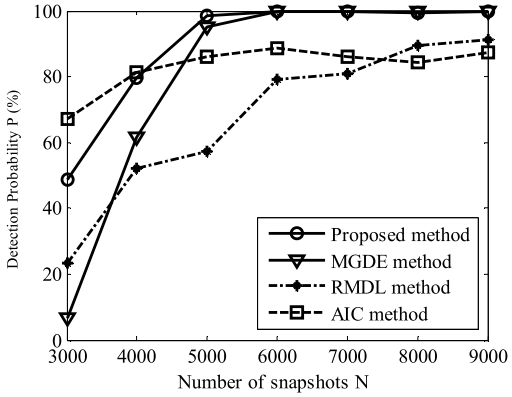

FIGURE 6. Detection probability of the number of SOIs as a function of the number of snapshots.

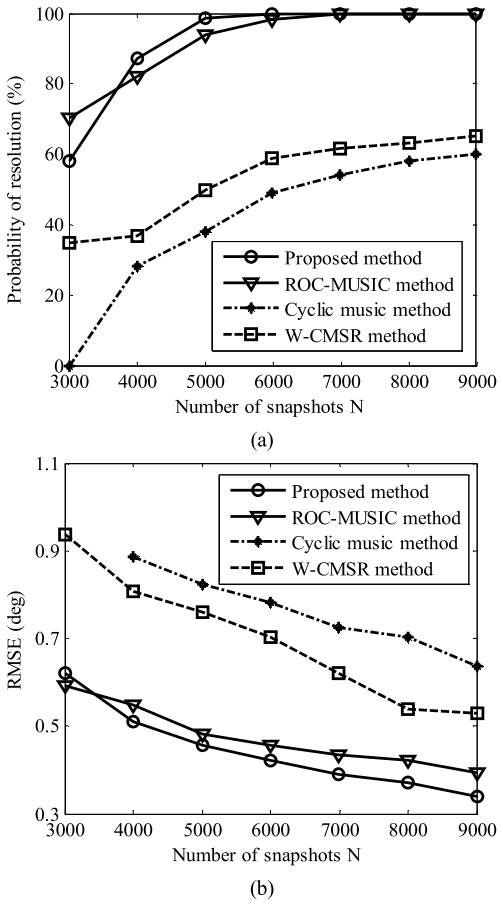

FIGURE 7. Probability of resolution (a) and RMSE (b) of DOA estimation as a function of the number of snapshots.

limited data is a very important parameter for an accurate DOA estimation.

B. COMPARATIVE EXPERIMENTS UNDER DIFFERENT CONDITIONS

Example A (Performance Versus Kernel Size): As the kernel size is a crucial parameter in the MCC [37], this section discusses the performance of the proposed method regarding the kernel size. The simulation conditions are the same as those described in the previous experiment, except that the kernel size varies from 0.1 to 2.9. Fig. 5 shows the probability of success and the RMSE of the DOA estimation versus the kernel size. From Fig. 5, we can observe that $\rho \in [1.2, 1.6]$ would be the optimal domain for the proposed algorithm to achieve the best performance. Therefore, in subsequent simulation experiments, the kernel size is set at $\rho = 1.5$.

Example B (Performance Versus Number of Snapshots): The number of snapshots is an important parameter that determines the performance of the DOA and the number of SOIs estimation. The simulation conditions are the same as those described in the previous experiment, except that the number of snapshots N varies from 3000 to 9000. Fig. 6 shows the detection probability of the number of SOIs versus the number of snapshots. As the proposed algorithm requires a long data length in order to induce cyclostationarity and reduce the estimation error, it is inferior to the AIC method but is superior to other algorithms when $N \geq 4000$. In addition, since the second-order statistics cannot suppress the impulse noise, the RMDL and AIC methods cannot achieve a high estimate accuracy. Fig. 7 evaluates the resolution

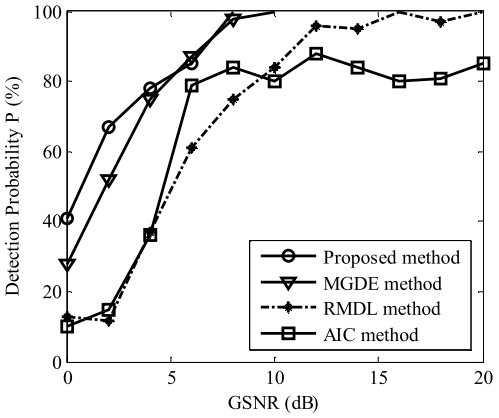

FIGURE 8. Detection probability of the number of SOIs as a function of the GSNR.

probability and the RMSE of the DOA estimation. As illustrated in Fig. 7, the performance of the proposed algorithm is more sensitive to less snapshots ($N < 4000$) than ROC-MUSIC but is superior to other algorithms when the number of snapshots $N \geq 4000$.

Example C (Performance Versus GSNR): In this experiment, we analyze the influence of the GSNR on the performance of the proposed algorithm. The simulation conditions are the same as those in the first example, except that the GSNRs vary from −3dB to 15dB in 2dB steps. Fig. 8 shows the detection probability of the number of SOIs versus the GSNR. As shown, the proposed algorithm has better estimation of the number of SOIs for relatively low GSNRs. Fig. 9 evaluates the resolution probability and the RMSE of the three algorithms for the DOA estimation versus the GSNR. The figure indicates that the performance of the proposed approach is superior to that of other algorithms, even with a low SNR. From the example, we can see that the proposed algorithm is relatively insensitive to the GSNR because the variation of non-cyclic impulsive noise does not appear in the cyclic frequency at $\varepsilon \neq 0$.

Example D (Performance Versus Characteristic Exponent): In this experiment, we study the influence of the characteristic exponent α to the detection and estimation performances. The parameters for the experiment are the same as the first example, except that the noise environments vary from serious impulsive (α is approximately 1) to Gaussian environments (α=2). Fig. 10 shows detection probability of the number of SOIs versus the characteristic exponent α. Note that for $\alpha \leq 1.1$ the RMDL and AIC methods cannot detect the number of SOIs in any of the 200 Monte Carlo runs. The results suggest that in impulsive noise environments modeled under the stable law, the performance of the traditional detection algorithm using second-order statistics is poor. With an increase in α, the detection probabilities of all algorithms are improved. Fig. 11 illustrates the performance of the four algorithms for DOA estimation in a wide range of noise environments. We note that for $\alpha < 1.2$, W-CMSR and cyclic MUSIC do not resolve the SOIs,

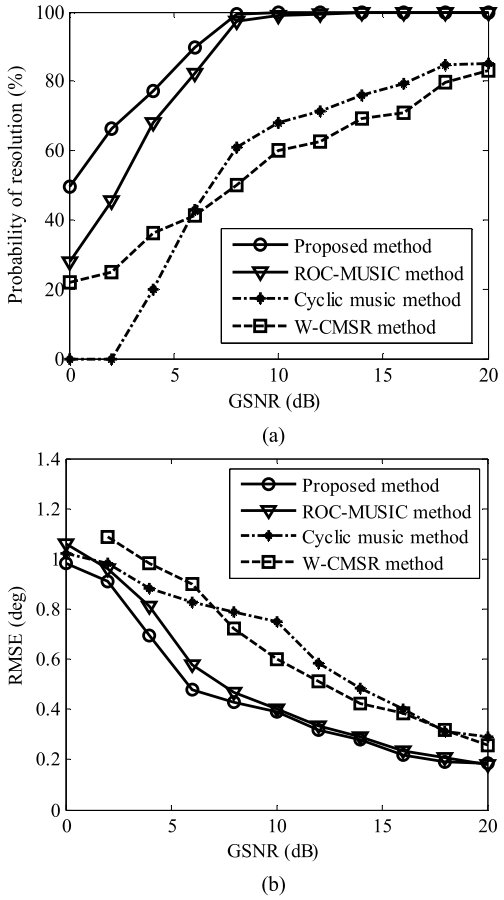

FIGURE 9. Probability of resolution (a) and RMSE (b) of DOA estimation as a function of the GSNR.

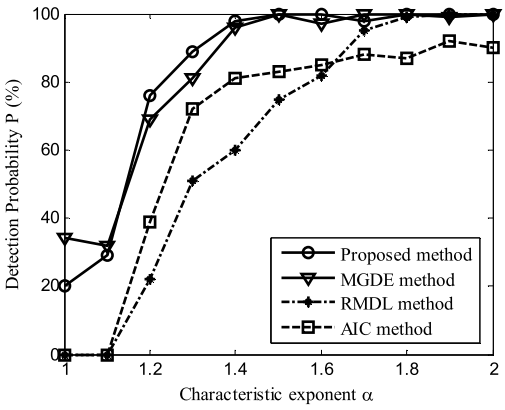

FIGURE 10. Detection probability of the number of SOIs as a function of the characteristic exponent α.

which suggests that the lower order moments or correntropy is more beneficial than the covariance matrix in impulsive noise environments. The performance of the proposed approach is improved over that of other three algorithms both in terms of the resolution probability and the RMSE for $\alpha \in [1, 2)$. Of course, for Gaussian additive noise ($\alpha = 2$), W-CMSR gives better results by use of the covariance matrix.

Example E (Performance Versus Angular Separation): We assume the two sources are the SOIs (BPSK) mentioned

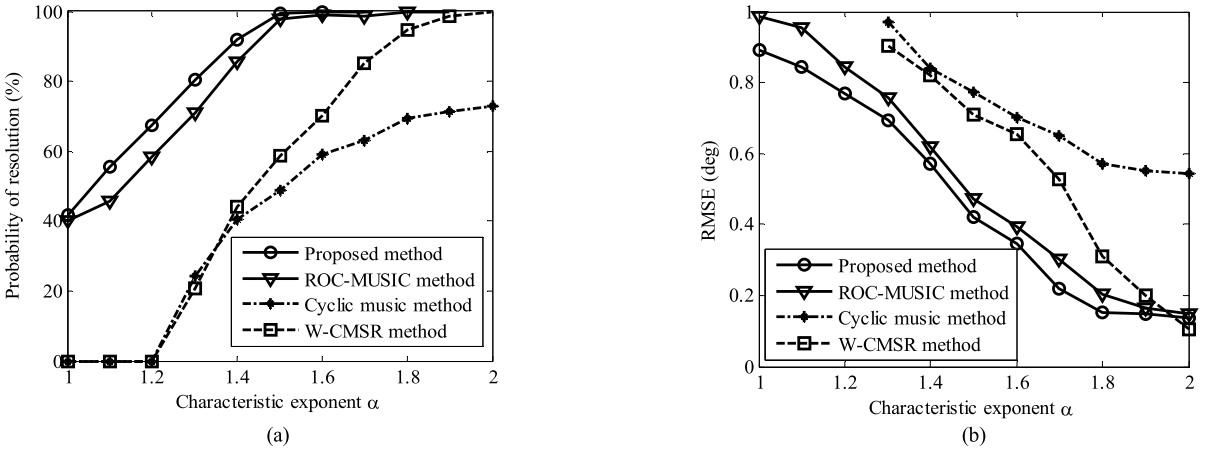

FIGURE 11. Probability of resolution (a) and RMSE (b) of the DOA estimation as a function of the characteristic exponent α.

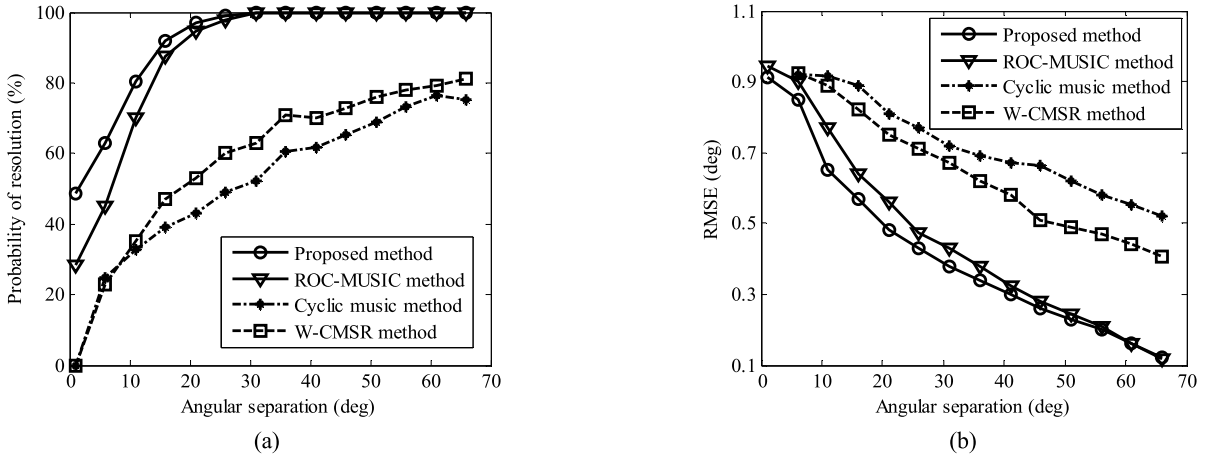

FIGURE 12. Probability of resolution (a) and RMSE (b) of the DOA estimation as a function of the angular separation.

above arriving from $\theta_1 = 4°$ and $\theta_2 = 4° + \Delta\theta$, where the angular separation $\Delta\theta$ varies from 1° to 66° in 1° steps, and the rest of the conditions are identical to those in the above examples. Fig. 12 illustrates the resolution probability and the RMSE of the DOA estimation versus $\Delta\theta$. As expected, the resolution capabilities of all algorithms are improved with an increase in the angle separation between the two SOIs. The figure shows that the estimation performance of the proposed algorithm is better than other algorithms because the information on the eigenvalues and eigenvectors is jointly exploited in the paper.

VI. CONCLUSIONS

In this paper, we investigate the joint DOA and sources number estimation for wideband signals in impulsive noise environments. By building the LP model of the CCF of the array signals, a CLS-based cyclic correntropy DOA estimation approach is proposed in a limited number of snapshots. To achieve a more accurate joint estimate of the DOA and the number of SOIs, we further develop an MCC-based iterative approach. The improved performance of the proposed algorithm is demonstrated via sufficient experiments. Simulations indicate the effectiveness of the proposed method for the DOA and the number of SOI estimations under the circumstances of co-channel interferences, limited snapshots, low GSNR and wide range of impulsive noise environments.

APPENDIX

A. PROOF OF LEMMA

From the definition of CCF in (3) and the data model in (7), the CCF of the $(M-i)$ th received signal for $i=1,\cdots,M-1$ can be obtain as follows

$$\begin{aligned} v^{\varepsilon}_{y_{M-i}}(\tau) &= \left\langle \kappa\left(y_{M-i}(t+\tau/2) - y_{M-i}(t-\tau/2)\right) e^{-j2\pi\varepsilon t}\right\rangle_t \\ &= \left\langle \sum_{k=1}^{K_\varepsilon} \kappa\left[x_k\left(t+\tau/2+\upsilon_{(M-i)k}\right) - x_k\left(t-\tau/2\right.\right.\right. \\ &\quad \left.\left.\left. +\upsilon_{(M-i)k}\right) e^{-j2\pi\varepsilon t}\right]\right\rangle_t \\ &= \sum_{k=1}^{K_\varepsilon} v^{\varepsilon}_{x_k}(\tau)\, e^{j2\pi\varepsilon\upsilon_{(M-i)k}} \end{aligned} \tag{53}$$

We can rewrite (53) as

$$v^{\varepsilon}_{y_{M-i}}(\tau) = \left(\boldsymbol{\Psi}^{\varepsilon}_{x_k}(\tau)\right)^{\mathrm{T}} \mathbf{p}_i \tag{54}$$

where

$$\mathbf{p}_i = \left[e^{j2\pi\varepsilon\upsilon_{(M-i)1}}, e^{j2\pi\varepsilon\upsilon_{(M-i)2}}, \cdots, e^{j2\pi\varepsilon\upsilon_{(M-i)K_\varepsilon}}\right]^{\mathrm{T}},$$
$$\boldsymbol{\Psi}^{\varepsilon}_{x_k}(\tau) = \left[v^{\varepsilon}_{x_1}(\tau), v^{\varepsilon}_{x_2}(\tau), \cdots, v^{\varepsilon}_{x_K}(\tau)\right]^{\mathrm{T}}.$$

Setting i to be $i = 1, \cdots, M-1$, yields the vector $\boldsymbol{\varphi}^{\varepsilon}_{y_{M-i}}(\tau) = \left[v^{\varepsilon}_{y_{M-1}}(\tau), v^{\varepsilon}_{y_{M-2}}(\tau), \cdots, v^{\varepsilon}_{y_1}(\tau)\right]^{\mathrm{T}}$ as follows

$$\boldsymbol{\varphi}^{\varepsilon}_{y_{M-i}}(\tau) = \left(\boldsymbol{\psi}^{\varepsilon}_{x_k}(\tau)\right)^{\mathrm{T}} \mathbf{P} \tag{55}$$

where $\mathbf{P} = [\mathbf{p}_1, \mathbf{p}_2, \ldots, \mathbf{p}_{M-1}] \in \mathbb{C}^{K_\varepsilon \times (M-1)}$.

As the matrix $\boldsymbol{\Phi} = \left[\boldsymbol{\varphi}^{\varepsilon}_{y_{M-i}}(0), \boldsymbol{\varphi}^{\varepsilon}_{y_{M-i}}(1), \cdots, \boldsymbol{\varphi}^{\varepsilon}_{y_{M-i}}(N-1)\right]^{\mathrm{T}}$, we further obtain the compact matrix-matrix form as

$$\boldsymbol{\Phi} = \boldsymbol{\Psi}\mathbf{P} \tag{56}$$

where $\boldsymbol{\Psi} = \left[\boldsymbol{\Psi}^{\varepsilon}_{x_k}(0), \cdots, \boldsymbol{\Psi}^{\varepsilon}_{x_k}(N-1)\right]^{\mathrm{T}}$, and rank $(\boldsymbol{\Psi}) = K_\varepsilon$.

Since the matrix $\mathbf{P}$ is a Vandermonde matrix and we assume M–1 $> K_\varepsilon$, we can obtain rank $(\mathbf{P}) = \min(M-1, K_\varepsilon) = K_\varepsilon$. Hence, we have rank $(\boldsymbol{\Phi}) = K_\varepsilon$, i.e., the rank of the matrix $\boldsymbol{\Sigma} = \boldsymbol{\Phi}^{\mathrm{H}}\boldsymbol{\Phi}$ is given by rank $(\boldsymbol{\Sigma}) = K_\varepsilon$.

B. PROOF OF THEOREM 2

From the defined MCC of the estimate $\hat{\mathbf{q}}_{\sigma^2,p}$ in (30), we obtain

$$\begin{aligned}\mathrm{MCC} &= E\left[\kappa\left(\hat{\mathbf{q}}_{\sigma^2,p} - \mathbf{q}\right)\right] \\ &= E\left[\frac{1}{\sqrt{2\pi}\rho}\exp\left\{-\frac{\Delta\mathbf{q}^2}{2\rho^2}\right\}\right]\end{aligned} \tag{57}$$

where $\Delta\mathbf{q} = \hat{\mathbf{q}}_{\sigma^2,p} - \mathbf{q}$.

For calculating the MCC defined in (57), it is necessary to calculate the correntropy matrix of the estimation error of the estimate $\hat{\mathbf{q}}_{\sigma^2,p}$. Based on (28), the error $\Delta\mathbf{q}$ in (57) can be obtained by

$$\begin{aligned}\Delta\mathbf{q} &= \hat{\mathbf{q}}_{\sigma^2,p} - \mathbf{q} \\ &= \left(\hat{\boldsymbol{\Phi}}^{\mathrm{H}}\hat{\boldsymbol{\Phi}} - \sigma^2\mathbf{I}_{M-1} + \mathbf{P}\right)^{-1}\hat{\boldsymbol{\eta}} - \mathbf{q} \\ &= \left(\hat{\boldsymbol{\Phi}}^{\mathrm{H}}\hat{\boldsymbol{\Phi}} - \sigma^2\mathbf{I}_{M-1} + \mathbf{P}\right)^{-1}\hat{\boldsymbol{\Phi}}^{\mathrm{H}}\left(\hat{\boldsymbol{\Phi}}q + \boldsymbol{\Delta\Psi}w\right) - \mathbf{q}\end{aligned} \tag{58}$$

Let $\mathbf{P}_0 = [\mathbf{O}_{M\times 1}, \mathbf{P}]$, $\hat{\boldsymbol{\Phi}}_0 = \left[\mathbf{O}_{M\times 1}, \hat{\boldsymbol{\Phi}}\right]$, then (57) can be rewritten as follows

$$\begin{aligned}\Delta\mathbf{q} &= \left(\hat{\boldsymbol{\Phi}}^{\mathrm{H}}\hat{\boldsymbol{\Phi}} - \sigma^2\mathbf{I}_{M-1} + \mathbf{P}\right)^{-1}\left[\left(-\hat{\boldsymbol{\Phi}}^{\mathrm{H}}\hat{\boldsymbol{\Phi}}_0 + \hat{\boldsymbol{\Phi}}^{\mathrm{H}}\boldsymbol{\Delta\Psi}\right)\right. \\ &\quad \left. + \left(\hat{\boldsymbol{\Phi}}^{\mathrm{H}}\hat{\boldsymbol{\Phi}} - \sigma^2\mathbf{I}_M + \mathbf{P}_0\right)\right]\mathbf{w} \\ &= \left(\hat{\boldsymbol{\Phi}}^{\mathrm{H}}\hat{\boldsymbol{\Phi}} - \sigma^2\mathbf{I}_{M-1} + \mathbf{P}\right)^{-1}\left(\hat{\boldsymbol{\Phi}}^{\mathrm{H}}\boldsymbol{\Delta\Psi} - \sigma^2\mathbf{I}_{M-1} + \mathbf{P}_0\right)\mathbf{w}\end{aligned} \tag{59}$$

Next, we obtain the error covariance matrix of the estimate $\hat{\mathbf{q}}_{\sigma^2,p}$ as follows (details shown in [18])

$$\begin{aligned}J_a &= \lim_{N\to\infty}\left[\boldsymbol{\Delta}\mathbf{q}\left(\boldsymbol{\Delta}\mathbf{q}\right)^{\mathrm{H}}\right] \\ &= \lim_{N\to\infty}\left\{\left(\hat{\mathbf{q}}_{\sigma^2,p} - \mathbf{q}\right)\left(\hat{\mathbf{q}}_{\sigma^2,p} - \mathbf{q}\right)^{\mathrm{H}}\right\} \\ &= \frac{1}{N}\left(\hat{\boldsymbol{\Phi}}^{\mathrm{H}}\hat{\boldsymbol{\Phi}} - \sigma^2\mathbf{I}_{M-1} + \mathbf{P}\right)^{-1}\left[\sigma^2\left(1 + \|\mathbf{q}\|^2\right)\hat{\boldsymbol{\Phi}}^{\mathrm{H}}\hat{\boldsymbol{\Phi}}\right. \\ &\quad \left. + \sigma^4\mathbf{q}\mathbf{q}^{\mathrm{H}} + N\mathbf{P}\mathbf{q}\mathbf{q}^{\mathrm{H}}\mathbf{P}\right]\left(\hat{\boldsymbol{\Phi}}^{\mathrm{H}}\hat{\boldsymbol{\Phi}} - \sigma^2\mathbf{I}_{M-1} + \mathbf{P}\right)^{-1}\end{aligned} \tag{60}$$

From the fact that

$$\mathrm{MCC} = E\left[\frac{1}{\sqrt{2\pi}\rho}\exp\left\{-\frac{\mathrm{diag}\,(J_a)}{2\rho^2}\right\}\right] \tag{61}$$

where

$$\begin{aligned}&\mathrm{diag}\,(J_a) \\ &= \frac{\sigma^2}{N}\left(1 + \|\mathbf{q}\|^2\right) \times \mathrm{diag}\left[\hat{\boldsymbol{\Phi}}^{\mathrm{H}}\hat{\boldsymbol{\Phi}}\left(\hat{\boldsymbol{\Phi}}^{\mathrm{H}}\hat{\boldsymbol{\Phi}} - \sigma^2\mathbf{I}_{M-1} + \mathbf{P}\right)^{-2}\right. \\ &\quad + \sigma^2\mathbf{q}\left(\hat{\boldsymbol{\Phi}}^{\mathrm{H}}\hat{\boldsymbol{\Phi}} - \sigma^2\mathbf{I}_{M-1} + \mathbf{P}\right)^{-2}\mathbf{q}^{H} \\ &\quad \left. + N\mathbf{q}^{\mathrm{H}}\mathbf{P}^{\mathrm{H}}\left(\hat{\boldsymbol{\Phi}}^{\mathrm{H}}\hat{\boldsymbol{\Phi}} - \sigma^2\mathbf{I}_{M-1} + \mathbf{P}\right)^{-2}\mathbf{P}\mathbf{q}\right] \\ &= \left[\frac{\sigma^2\hat{\lambda}_1\left(1 + \|\mathbf{q}\|^2\right) + \sigma^4\left|\hat{\mathbf{u}}_1^{\mathrm{H}}\mathbf{q}\right|^2 + N\gamma_1^2\left|\hat{\mathbf{u}}_1^{\mathrm{H}}\mathbf{q}\right|^2}{N\left(\hat{\lambda}_1 - \sigma^2 + \gamma_1\right)^2}, \cdots,\right. \\ &\quad \left.\frac{\sigma^2\hat{\lambda}_{M-1}\left(1 + \|\mathbf{q}\|^2\right) + \sigma^4\left|\hat{\mathbf{u}}_{M-1}^{\mathrm{H}}\mathbf{q}\right|^2 + N\gamma_{M-1}^2\left|\hat{\mathbf{u}}_{M-1}^{\mathrm{H}}\mathbf{q}\right|^2}{N\left(\hat{\lambda}_{M-1} - \sigma^2 + \gamma_{M-1}\right)^2}\right]\end{aligned}$$

We finally obtain the asymptotic MCC in (33)

$$\begin{aligned}\mathrm{MCC}\left(\{\gamma_i\}\right) = \frac{1}{\sqrt{2\pi}\rho}\sum_{i=1}^{M-1}\exp\left\{-\frac{\sigma^2\hat{\lambda}_i\left(1 + \|\mathbf{q}\|^2\right)}{2\rho^2 N\left(\hat{\lambda}_i - \sigma^2 + \gamma_i\right)^2}\right. \\ \left. - \frac{\sigma^4\left|\hat{\mathbf{u}}_i^{\mathrm{H}}\mathbf{q}\right|^2 + N\gamma_i^2\left|\hat{\mathbf{u}}_i^{\mathrm{H}}\mathbf{q}\right|^2}{2\rho^2 N\left(\hat{\lambda}_i - \sigma^2 + \gamma_i\right)^2}\right\}\end{aligned} \tag{62}$$

REFERENCES

[1] T. Chen, L. Shi, and L. Guo, "Sparse DOA estimation algorithm based on fourth-order cumulants vector exploiting restricted non-uniform linear array," *IEEE Access*, vol. 7, pp. 9980–9988, 2018.

[2] R. O. Schmidt, "Multiple emitter location and signal parameter estimation," *IEEE Trans. Antennas Propag.*, vol. AP-34, no. 3, pp. 276–280, Mar. 1986.

[3] R. Roy, A. Paulraj, and T. Kailath, "ESPRIT—A subspace rotation approach to estimation of parameters of cisoids in noise," *IEEE Trans. Acoust., Speech, Signal Process.*, vol. 34, no. 5, pp. 1340–1342, Oct. 1986.

[4] D. W. Tufts and R. Kumaresan, "Estimation of frequencies of multiple sinusoids: Making linear prediction perform like maximum likelihood," *Proc. IEEE*, vol. 70, no. 9, pp. 975–989, Sep. 1982.

[5] P. Stoica and K. C. Sharman, "Novel eigenanalysis method for direction estimation," *IEE Proc. F Radar Signal Process.*, vol. 137, no. 1, pp. 19–26, Feb. 1990.

[6] T. Bai, C. Xu, R. Zhang, A. F. Al Rawi, and L. Hanzo, "Performance of HARQ-assisted OFDM systems contaminated by impulsive noise: Finite-length LDPC code analysis," *IEEE Access*, vol. 7, pp. 14112–14123, 2019.

[7] P. Tsakalides and C. L. Nikias, "The robust covariation-based MUSIC (ROC-MUSIC) algorithm for bearing estimation in impulsive noise environments," *IEEE Trans. Signal Process.*, vol. 44, no. 7, pp. 1623–1633, Jul. 1996.

[8] T.-H. Liu and J. M. Mendel, "A subspace-based direction finding algorithm using fractional lower order statistics," *IEEE Trans. Signal Process.*, vol. 49, no. 8, pp. 1605–1613, Aug. 2001.
[9] S. Visuri, H. Oja, and V. Koivunen, "Subspace-based direction-of-arrival estimation using nonparametric statistics," *IEEE Trans. Signal Process.*, vol. 49, no. 9, pp. 2060–2073, Sep. 2001.
[10] P. Tsakalides and C. L. Nikias, "Wideband array signal processing with alpha-stable distributions," in *Proc. IEEE Conf. Rec. Mil. Commun. Conf. (MILCOM)*, vol. 1, Nov. 1995, pp. 135–139.
[11] G.-H. You, T.-S. Qiu, and A.-M. Song, "Novel direction findings for cyclostationary signals in impulsive noise environments," *Circuits, Syst. Signal Process.*, vol. 32, no. 6, pp. 2939–2956, 2013.
[12] L.-C. Zhao, P. Krishnaiah, and Z.-D. Bai, "Remarks on certain criteria for detection of number of signals," *IEEE Trans. Acoust., Speech, Signal Process.*, vol. 35, no. 2, pp. 129–132, Feb. 1987.
[13] M. Viberg, B. Ottersten, and T. Kailath, "Detection and estimation in sensor arrays using weighted subspace fitting," *IEEE Trans. Signal Process.*, vol. 39, no. 11, pp. 2436–2449, Nov. 1991.
[14] A. N. Manikas and L. F. Turner, "Adaptive signal parameter estimation and classification technique," *IEE Proc. F Radar Signal Process.*, vol. 138, no. 3, pp. 267–277, Jun. 1991.
[15] Q. Chong-Ying, Z. Yong-Shun, H. A. N. Ying, and C. Xi-Hong, "An algorithm on high resolution DOA estimation with unknown number of signal sources," in *Proc. 4th Int. Conf. Microw. Millim. Wave Technol. (ICMMT)*, no. 2, Aug. 2004, pp. 227–230.
[16] C.-S. Park, J.-H. Choi, J.-W. Yang, and S.-P. Nah, "Direction of arrival estimation using weighted subspace fitting with unknown number of signal sources," in *Proc. 11th Int. Conf. Adv. Commun. Technol. (ICACT)*, vol. 3, Feb. 2009, pp. 2295–2298.
[17] V. V. Reddy, M. Mubeen, and B. P. Ng, "Reduced-complexity super-resolution DOA estimation with unknown number of sources," *IEEE Signal Process. Lett.*, vol. 22, no. 6, pp. 772–776, Jun. 2015.
[18] J. Xin and A. Sano, "MSE-based regularization approach to direction estimation of coherent narrowband signals using linear prediction," *IEEE Trans. Signal Process.*, vol. 49, no. 11, pp. 2481–2497, Nov. 2001.
[19] P. Wang, T.-S. Qiu, F.-Q. Ren, and A.-M. Song, "A robust DOA estimator based on the correntropy in alpha-stable noise environments," *Digit. Signal Process.*, vol. 60, pp. 242–251, Jan. 2017.
[20] A. I. R. Fontes, J. B. A. Rego, A. M. de Martins, L. F. Q. Silveira, and J. C. Principe, "Cyclostationary correntropy: Definition and applications," *Expert Syst. Appl.*, vol. 69, pp. 110–117, Mar. 2017.
[21] B. Chen, X. Liu, and H. Zhao, "Maximum correntropy Kalman filter," *Automatica*, vol. 76, pp. 70–77, Feb. 2017.
[22] S. Y. Luan, T. Qiu, Y. Zhu, and L. Yu, "Cyclic correntropy and its spectrum in frequency estimation in the presence of impulsive noise," *Signal Process.*, vol. 120, pp. 503–508, Mar. 2016.
[23] T. Liu, T. Qiu, and S. Luan, "Cyclic correntropy: Foundations and theories," *IEEE Access*, vol. 6, pp. 34659–34669, 2018.
[24] R. Kapoor, A. Banerjee, G. A. Tsihrintzis, and N. Nandhakumar, "UWB radar detection of targets in foliage using alpha-stable clutter models," *IEEE Trans. Aerosp. Electron. Syst.*, vol. 35, no. 3, pp. 819–834, Jul. 1999.
[25] P. G. Georgiou, P. Tsakalides, and C. Kyriakakis, "Alpha-stable modeling of noise and robust time-delay estimation in the presence of impulsive noise," *IEEE Trans. Multimedia*, vol. 1, no. 3, pp. 291–301, Sep. 1999.
[26] R. Roy and T. Kailath, "Esprit-estimation of signal parameters via rotational invariance techniques," *IEEE Trans. Acoust., Speech, Signal Process.*, vol. 37, no. 7, pp. 984–995, Jul. 1989.
[27] J. Yin and T. Chen, "Direction-of-arrival estimation using a sparse representation of array covariance vectors," *IEEE Trans. Signal Process.*, vol. 59, no. 9, pp. 4489–4493, Sep. 2011.
[28] D. Malioutov, M. Çetin, and A. S. Willsky, "A sparse signal reconstruction perspective for source localization with sensor arrays," *IEEE Trans. Signal Process.*, vol. 53, no. 8, pp. 3010–3022, Aug. 2005.
[29] G. Xu and T. Kailath, "Direction-of-arrival estimation via exploitation of cyclostationary—A combination of temporal and spatial processing," *IEEE Trans. Signal Process.*, vol. 40, no. 7, pp. 1775–1786, Jul. 1992.
[30] M. D. Rahman and K.-B. Yu, "Total least squares approach for frequency estimation using linear prediction," *IEEE Trans. Acoust., Speech, Signal Process.*, vol. ASSP-35, no. 10, pp. 1440–1454, Oct. 1987.
[31] W. Liu, P. P. Pokharel, and J. C. Principe, "Correntropy: Properties and applications in non-Gaussian signal processing," *IEEE Trans. Signal Process.*, vol. 55, no. 11, pp. 5286–5298, Nov. 2007.
[32] B. Chen, J. Wang, H. Zhao, N. Zheng, and J. C. Príncipe, "Convergence of a fixed-point algorithm under maximum correntropy criterion," *IEEE Signal Process. Lett.*, vol. 22, no. 10, pp. 1723–1727, Oct. 2015.
[33] E. Fishler and H. V. Poor, "Estimation of the number of sources in unbalanced arrays via information theoretic criteria," *IEEE Trans. Signal Process.*, vol. 53, no. 9, pp. 3543–3553, Sep. 2005.
[34] H.-T. Wu, J.-F. Yang, and F.-K. Chen, "Source number estimators using transformed Gerschgorin radii," *IEEE Trans. Signal Process.*, vol. 43, no. 6, pp. 1325–1333, Jun. 1995.
[35] Z. M. Liu, Z. T. Huang, and Y. Y. Zhou, "Direction-of-arrival estimation of wideband signals via covariance matrix sparse representation," *IEEE Trans. Signal Process.*, vol. 59, no. 9, pp. 4256–4270, Sep. 2011.
[36] M. Kaveh and A. J. Barabell, "The statistical performance of the MUSIC and the minimum-norm algorithms in resolving plane waves in noise," *IEEE Trans. Acoust., Speech, Signal Process.*, vol. ASSP-34, no. 2, pp. 331–341, Apr. 1986.
[37] B. Chen, L. Xing, B. Xu, H. Zhao, N. Zheng, and J. C. Principe. (2016). "Kernel risk-sensitive loss: Definition, properties and application to robust adaptive filtering." [Online]. Available: https://arxiv.org/abs/1608.00441

FANGXIAO JIN was born in Liaoning, China. She received the B.Sc. degree in electronic and information engineering from Liaoning Normal University, in 2014. She is currently pursuing the Ph.D. degree in signal and information processing with the Dalian University of Technology, Dalian, China. She has been with the SRMC-DUT Joint Laboratory of Radio Frequency Signal Processing, since 2014. Her research interests include wireless signal processing and array signal processing.

TIANSHUANG QIU received the B.S. degree from Tianjin University, Tianjin, China, in 1983, the M.S. degree from the Dalian University of Technology, Dalian, Liaoning, China, in 1993, and the Ph.D. degree from Southeastern University, Nanjing, China, in 1996, all in electrical engineering. He was a Postdoctoral Fellow with the Department of Electrical Engineering, Northern Illinois University, USA, from 1996 to 2000. He is currently a Professor with the Faculty of Electronic Information and Electrical Engineering, Dalian University of Technology. His research interests include wireless signal processing, biomedical signal processing, and non-Gaussian signal processing.

SHENGYANG LUAN received the B.Sc. degree from the Department of Electronic Engineering and Information Science, University of Science and Technology of China, Hefei, Anhui, China, in 2006, and the Ph.D. degree from the School of Information and Communication Engineering, Dalian University of Technology, Dalian, Liaoning, China, in 2017. Since 2017, he has been a Lecturer with the Institute of Electrical Engineering and Automation, Jiangsu Normal University, Xuzhou, Jiangsu, China. His research interests include non-Gaussian signal processing, nonstationary signal processing, adaptive signal processing, spatial signal processing, and machine learning.

WEI CUI was born in Liaoning, China. He received the B.Sc. degree in electronic and information engineering from Liaoning Normal University, Dalian, Liaoning, in 2013. He was a Hardware Engineer with Dalian Huaxin Computer Technology Co., Ltd., Liaoning, from 2013 to 2016. He is currently a Project Manager with Automotive Electronics, Neusoft Corporation, Dalian.